*Progress In Electromagnetics Research M, Vol. 73, 119–129, 2018*

# A New Adaptive Tracking Algorithm for Near-Space Hypersonic Target

**Xiangke Guo[1, *], Changyun Liu[2], Qiang Fu[2], and Gang Wang[2]**

**Abstract**—Because of the maneuvering of hypersonic target, the tracking of near space hypersonic targets is difficult. In this paper, a new adaptive tracking algorithm based on an aerodynamic model and improved square root cubature Kalman filter is proposed. The adaptive piecewise constant jerk model gives the acceleration recursive process based on the dynamic model. Considering the nonlinear characteristic of both the target state model and the observation model, the improved square-root cubature Kalman filter is applied to estimate the target state. The simulation results under different maneuvers conditions indicate that the proposed method has a higher degree of accuracy than the original aerodynamic model. The research provides a feasible solution to the further improvement of the real time tracking accuracy of near space hypersonic targets.

## 1. INTRODUCTION

As projects related to near space hypersonic targets (NSHT) [1–3] developed by the U.S. forces gradually mature, NSHT with characteristics of expansive flight cross-domain, high velocity and complex aerodynamic parameter variation pose a challenge to the intercept and attack abilities of air defense and anti-missile systems [4–6]. Many studies have been conducted that deal with the motion modeling and tracking algorithm of NSHT. At present, the dynamic model based on a gravity turning frame and aerodynamic pressure is widely used for space targets and ballistic targets [7]. Wu and Chen used the aerodynamic model to estimate the motion state along with aerodynamic parameters [8]. However, the model has complex interactions and requires a large computational load. According to the dynamic characteristics of the air-breathing hypersonic target Li et al. proposed the dynamic hybrid model set for target tracking [9]. However, the analytical solution structure is difficult to implement for a linear filter design. To address the shortcomings of the traditional dynamic, Zhai et al. proposed a new aerodynamic model to realize the trajectory prediction of a hypersonic target. However, since no aerodynamic acceleration recursive step is given, the model cannot be directly used for filtering [10, 11].

Therefore, on the basis of the aerodynamic model in papers [10] and [11], a piecewise adaptive jerk tracking model of NSHT is proposed. The square root cubature Kalman filter (SRCKF) is used to accomplish the filter tracking of a target. This filter has better nonlinear approximation features, numerical accuracy, small computation and suitability for real-time calculation [12–14]. Finally, the effectiveness of the new adaptive tracking algorithm is verified by simulation.

## 2. THE DYNAMIC MODEL OF NSHT

The acceleration model of a maneuvering reentry target can be written as [7]:

$$\frac{d^2\mathbf{r}}{dt^2} = \mathbf{a} + \mathbf{g} - \boldsymbol{\omega}_\mathbf{e} \times (\boldsymbol{\omega}_\mathbf{e} \times \mathbf{r}) - 2\boldsymbol{\omega}_\mathbf{e} \times \mathbf{v} \tag{1}$$

*Received 1 July 2018, Accepted 4 September 2018, Scheduled 19 September 2018*

* Corresponding author: Xiangke Guo (guosyanyu@163.com).

[1] School of Electronic and Information Engineering, Beihang University, China. [2] Air Force Engineering University, China.

where $\mathbf{r}$, $\mathbf{v}$, $\mathbf{g}$, $\omega_e$ and $\mathbf{a}$ indicate the earth vector of a target, flight speed of a target, gravity acceleration, earth rotation angular speed and aerodynamic acceleration. Also, $-\boldsymbol{\omega}_\mathbf{e} \times (\boldsymbol{\omega}_\mathbf{e} \times \mathbf{r})$ indicates inertial centripetal acceleration, and $-2\boldsymbol{\omega}_\mathbf{e} \times \mathbf{v}$ indicates Coriolis acceleration.

The aerodynamic acceleration $\mathbf{a}$ is the main factor affecting the maneuver of the target, and its change determines the maneuvering state of the aircraft. Therefore, the inertial centripetal acceleration and Coriolis acceleration in the total target acceleration can be ignored. The gravity acceleration $\mathbf{g}$ can be respectively modeled as a flat model, ball model and ellipsoid model. Here, focus on the modeling of aerodynamic acceleration $\mathbf{a}$.

## 3. PIECEWISE-CONSTANT JERK MODEL

### 3.1. The Piecewise-Constant Acceleration Model

According to the concept of piecewise uniform acceleration (Piecewise-Constant Acceleration, or PCA) [7], under an ENU coordinate system, using aerodynamics parameter $\boldsymbol{\alpha}_{\mathrm{VTC}}$ model aerodynamics acceleration can be stated as [10]:

$$\begin{cases} \ddot{x} = \alpha_V P_0 \dot{x} - \alpha_T P_0 v \dfrac{\dot{y}}{v_g} - \alpha_C P_0 \dfrac{\dot{x}\dot{z}}{v_g} \\ \ddot{y} = \alpha_V P_0 \dot{y} + \alpha_T P_0 v \dfrac{\dot{x}}{v_g} \alpha_t - \alpha_C P_0 \dfrac{\dot{y}\dot{z}}{v_g} \\ \ddot{z} = -\alpha_V P_0 \dot{z} + \alpha_C P_0 v_g - g \end{cases} \tag{2}$$

where $\ddot{x}_k$, $\ddot{y}_k$, $\ddot{z}_k$ are the acceleration components along the three axes in the ENU system; $P_0$ is the free flow of pressure; $\mathbf{v}$ is the target speed; $\boldsymbol{\alpha}_{VTC} = [\alpha_V, \alpha_T, \alpha_C]^T$ is the aerodynamics parameter. The relationship between the aerodynamic parameter $\boldsymbol{\alpha}_{VTC}$ and the acceleration of the target in the VTC coordinate system is $\mathbf{a}_{VTC} = [a_V; a_T; a_C\ ] = [\alpha_V P_0 v; \alpha_T P_0 v; \alpha_C P_0 v\ ]$.

From Eq. (2), it can be seen that the PCA model does not give a recursive equation for aerodynamic acceleration. In each filtering cycle, the target acceleration cannot be directly corrected using innovation. Therefore, if either the target maneuver or the initial state setting is inaccurate, the likelihood of a system tracking error will increase. When a recursive model of acceleration is established in the state equation, the state model can rectify the acceleration item recursively, according to the observational innovation of the sensor in each filtering period. That can improve the estimation accuracy of the system state. Therefore, in this paper, based on the previous aerodynamic model, the recursive equation of the target aerodynamic acceleration is established, and a piecewise constant Jerk adaptive tracking model for tracking hypersonic targets is proposed.

### 3.2. The Piecewise-Constant Jerk Model

Suppose that the jerk value of the NSHT is uniform in the sampling interval. According to random model approximate thought [15], taking random error into the acceleration recursion equation, the acceleration recursion equation is defined by:

$$\begin{bmatrix} \ddot{x}_{k+1} \\ \ddot{y}_{k+1} \\ \ddot{z}_{k+1} \end{bmatrix} = \begin{bmatrix} \ddot{x}_k \\ \ddot{y}_k \\ \ddot{z}_k \end{bmatrix} + \begin{bmatrix} \dddot{x}_k \\ \dddot{y}_k \\ \dddot{z}_k \end{bmatrix} T + \mathbf{w}_k \tag{3}$$

where $w_k$ is defined as the acceleration vector at time $k$ and the error which is generated by the random error of jerk acceleration at time $k+1$, $\mathbf{w}_k = \begin{bmatrix} \tilde{\ddot{x}}_k + \tilde{\dddot{x}}_k T & \tilde{\ddot{y}}_k + \tilde{\dddot{y}}_k T & \tilde{\ddot{z}}_k + \tilde{\dddot{z}}_k T \end{bmatrix}^T$.

From Eq. (3), the subsection uniform jerk model state equation under an ENU coordinate system is generated by

$$\mathbf{X}_{k+1} = \mathbf{F}_{CA} \mathbf{X}_k + \mathbf{G}_J J(\mathbf{X}_k, \mathbf{p}_k) + \mathbf{W}_k^{CJ} \tag{4}$$

where $\mathbf{X}_k = (x_k, \dot{x}_k, \ddot{x}_k, y_k, \dot{y}_k, \ddot{y}_k, z_k, \dot{z}_k, \ddot{z}_k)^T$ is the target state vector; $\mathbf{F}_{CA} = \mathrm{blkdiag}(F, F, F)$ is the state transition matrix; $\mathbf{G}_J = \mathrm{blkdiag}(\mathbf{G}_x, \mathbf{G}_y, \mathbf{G}_z)$ is the jerk input matrix, and $\mathbf{G}_x = \mathbf{G}_y = \mathbf{G}_z = \left[T^3/6, T^2/2, T\right]^T$; $\mathbf{p}_k$ is the aerodynamics parameter vector, which has the same meaning as in Eq. (4);

$J(\mathbf{X}_k, \mathbf{p}_k) = \begin{bmatrix} \dddot{x}_k & \dddot{y}_k & \dddot{z}_k \end{bmatrix}^T$ is the jerk of the target; $\mathbf{W}_k^{CJ}$ is the Gaussian noise of covariance matrix $\mathbf{Q}_k^{CJ}$; $\mathbf{Q}_k^{CJ} = \text{blkdiag}\left(\sigma_{ax}^2\mathbf{q}_{CA}, \sigma_{ay}^2\mathbf{q}_{CA}, \sigma_{az}^2\mathbf{q}_{CA}\right)$, $\sigma_{ax}^2$, $\sigma_{ay}^2$ and $\sigma_{az}^2$ are instantaneous variances of acceleration in the $x$, $y$ and $z$ directions, respectively. Also, $F$ and $\mathbf{q}_{CA}$ are defined as:

$$F = \begin{bmatrix} 1 & T & \frac{T^2}{2} \\ 0 & 1 & T \\ 0 & 0 & 1 \end{bmatrix}, \quad \mathbf{q}_{CA} = \begin{bmatrix} 0 & 0 & 0 \\ 0 & 0 & 0 \\ 0 & 0 & q_a T \end{bmatrix}$$

Where $q_a$ is the steady state precision adjust factor, according to Eq. (2), and $J(\mathbf{X}_k, \mathbf{p}_k)$ is computed by

$$\begin{cases} \dddot{x} = \alpha_V P_0 \ddot{x} - \alpha_T P_0 \left( \dot{v}\dfrac{\dot{y}}{v_g} + v\dfrac{\ddot{y}}{v_g} - v\dfrac{\dot{y}}{v_g^2}\dot{v}_g \right) - \alpha_C P_0 \left( \dfrac{\ddot{x}\dot{z}}{v_g} + \dfrac{\dot{x}\ddot{z}}{v_g} - \dfrac{\dot{x}\dot{z}}{v_g^2}\dot{v}_g \right) \\ \dddot{y} = \alpha_V P_0 \ddot{y} + \alpha_T P_0 \left( \dot{v}\dfrac{\dot{x}}{v_g} + v\dfrac{\ddot{x}}{v_g} - v\dfrac{\dot{x}}{v_g^2}\dot{v}_g \right) - \alpha_C P_0 \left( \dfrac{\ddot{y}\dot{z}}{v_g} + \dfrac{\dot{y}\ddot{z}}{v_g} - \dfrac{\dot{y}\dot{z}}{v_g^2}\dot{v}_g \right) \\ \dddot{z} = \alpha_V P_0 \ddot{z} + \alpha_C P_0 \dot{v}_g \end{cases} \tag{5}$$

where $v = \sqrt{\dot{x}^2 + \dot{y}^2 + \dot{z}^2}$ is the flight speed of the target, $v_g = \sqrt{\dot{x}^2 + \dot{y}^2}$, $\dot{v} = \frac{\dot{x}\ddot{x} + \dot{y}\ddot{y} + \dot{z}\ddot{z}}{v}$, $\dot{v}_g = \frac{\dot{x}\ddot{x} + \dot{y}\ddot{y}}{v_g}$.

Suppose $\boldsymbol{\sigma}_{ak}^2 = \begin{bmatrix} \sigma_{ax}^2 & \sigma_{ay}^2 & \sigma_{az}^2 \end{bmatrix}^T$, the instantaneous variance of acceleration is generated by

$$\boldsymbol{\sigma}_{ak}^2 = \text{diag}\left( [\tilde{\ddot{\mathbf{x}}}_k \tilde{\ddot{\mathbf{x}}}_k^T] + T^2 [\tilde{\dddot{\mathbf{x}}}_k \tilde{\dddot{\mathbf{x}}}_k^T] + 2T [\tilde{\ddot{\mathbf{x}}}_k \tilde{\dddot{\mathbf{x}}}_k^T] \right) \tag{6}$$

where $\tilde{\ddot{\mathbf{x}}}_k = \begin{bmatrix} \tilde{\ddot{x}}_k & \tilde{\ddot{y}}_k & \tilde{\ddot{z}}_k \end{bmatrix}^T$ is the acceleration estimation vector, and $\tilde{\dddot{\mathbf{x}}}_k = \begin{bmatrix} \tilde{\dddot{x}}_k & \tilde{\dddot{y}}_k & \tilde{\dddot{z}}_k \end{bmatrix}^T$ is the jerk estimation error vector. When ignoring the product of the jerk and acceleration error, the variance expectation of acceleration and jerk are similar to the instantaneous variance. Therefore, Eq. (6) can be defined by

$$\boldsymbol{\sigma}_{ak}^2 = \text{diag}\left( C_a E[\tilde{\ddot{\mathbf{x}}}_k \tilde{\ddot{\mathbf{x}}}_k^T] + T^2 C_J E[\tilde{\dddot{\mathbf{x}}}_k \tilde{\dddot{\mathbf{x}}}_k^T] \right) \tag{7}$$

where $C_a$ and $C_J$, respectively, are the acceleration and jerk variance conversion coefficient. The recursion of aerodynamic parameters in the segmented uniform jerk model can be achieved by separately calculating $E[\tilde{\ddot{\mathbf{x}}}_k \tilde{\ddot{\mathbf{x}}}_k^T]$ and $E[\tilde{\dddot{\mathbf{x}}}_k \tilde{\dddot{\mathbf{x}}}_k^T]$, using different filtering algorithms.

## 4. IMPROVED SQUARE ROOT CUBATURE KALMAN FILTER

### 4.1. Square Root Cubature Kalman Filter

Considering the nonlinear characteristics of the target state model and the observation model, the nonlinear approximation performance and numerical accuracy are better than those of other nonlinear filtering algorithms. The algorithm has a small computational load and is more suitable for real-time calculation. The cubature Kalman filter (CKF) has higher filtering precision than the Unscented Kalman filter (UKF) when the dimensionality of the target state is greater than 3. In the process of CKF, the error covariance matrices need to be decomposed and inverted. However, it is difficult to guarantee the positive definite of the error covariance matrix. Therefore, the state-filtering of the target is avoided by introducing Cholesky decomposition, in order to avoid the square root cubature Kalman filter (SRCKF), which directly performs the square root operation on the covariance matrix and has better filtering stability [12–14]. The SRCKF avoids the square root operation of the iterative matrix by introducing orthogonally triangular decomposition. However, the SRCKF directly calculates the square root of the covariance matrix. It solves the easy divergence issue of a conventional CKF algorithm and improves the accuracy and stability of filtering.

To realize the recursive estimation of the hypersonic target aerodynamic parameter $p$ in the adjacent space, the segment jerk model is extended as a state estimation parameter, and the extended jerk motion model is shown in Eq. (8), as follows:

$$\begin{bmatrix} \mathbf{X}_{k+1} \\ \mathbf{p}_{k+1} \end{bmatrix} = \begin{bmatrix} \mathbf{F}_J & 0 \\ 0 & \mathbf{I} \end{bmatrix} \begin{bmatrix} \mathbf{X}_k \\ \mathbf{p}_k \end{bmatrix} + \begin{bmatrix} \mathbf{G}_J \\ 0 \end{bmatrix} \mathbf{J}_k + \begin{bmatrix} \mathbf{W}_k^J \\ \mathbf{W}_{pk} \end{bmatrix} \tag{8}$$

where $\mathbf{W}_{pk}$ is the parameter of Wiener model process noise, and $\mathbf{Q}_{pk}$ is the covariance matrix. Combine Eq. (8) with the measure equation, and the result is as follows:

$$\begin{cases} \mathbf{X}_k^a = f(\mathbf{X}_{k-1}^a) + \mathbf{W}_{k-1}^a \\ \mathbf{Z}_k = h(\mathbf{X}_k^a) + \mathbf{V}_k \end{cases} \tag{9}$$

where $\mathbf{X}_{k-1}^a = \left(\mathbf{X}_{k-1}^T, \mathbf{p}_{k-1}^T\right)^T$; $\mathbf{W}_{k-1}^a = [(\mathbf{W}_{k-1}^J)^T, \mathbf{W}_{p,k-1}^T]^T$, $h(\mathbf{X}_k^a)$ is a nonlinear function between the measured value and the state value, and the measurement noise $\mathbf{V}_k$ is a zero-mean Gaussian white noise vector with variance $\mathbf{R}_k$.

Suppose the posterior probability distribution of the known state estimation is $p(\mathbf{x}_{k-1}^a|\mathbf{z}_{1:k-1}) \sim \mathrm{N}(\mathbf{x}_{k-1}^a; \hat{\mathbf{x}}_{k-1}^a, P_{k-1}^a)$, the corresponding covariance is $P_{k-1}^a$, and the expanded model progress noise covariance matrix is $\mathbf{Q}_k^a = \mathrm{blkdiag}(\mathbf{Q}_k^J, \mathbf{Q}_{pk})$; then $\mathbf{S}_{x,k}^a = \mathrm{chol}(\mathbf{P}_k^a)$ is a Cholesky decomposition. The SRCKF algorithm based on the expanded status model is defined as follows:

(1) Calculate the basic cubature points and the corresponding weights.

The nonlinear filtering problem under Gaussian distribution can be reduced to an integral calculus problem. The standard Gaussian weighted integral can be calculated by using the third-degree spherical radial rule and $2n_x$ volume points are needed. The basic cubature point and the corresponding weight is:

$$\xi_i = \sqrt{\frac{m}{2}}\,[1]_i\,, \quad w_i = \frac{1}{m}, \quad i = 1, 2, \ldots, m \tag{10}$$

where the cubature point number is $m$, $m = 2n_x$, and $n_x$ is the dimension of state; $[1]_i$ represents the $i$-th column of the complete symmetric point set [1].

(2) Time updates

Calculate the $m$ cubature points of the current state ($i = 1, 2, \ldots m$), $m = 2n$.

$$X_{i,k-1|k-1}^a = \mathbf{S}_{k-1|k-1}^a \xi_i + \hat{x}_{k-1|k-1}^a \tag{11}$$

Calculate the predicted value of the volume point through the nonlinear state transfer function.

$$X_{i,k|k-1}^{a(*)} = f(X_{i,k-1|k-1}^a) \tag{12}$$

Estimate the predicted state (SRCKF uses equal weights) in conjunction with the weights and volume point predictions.

$$\hat{x}_{k|k-1}^a = \frac{1}{m}\sum_{i=1}^{m} X_{i,k|k-1}^{a(*)} \tag{13}$$

The square root of the estimated covariance matrix:

$$\mathbf{S}_{k|k-1}^a = \mathrm{Tria}([\boldsymbol{\chi}_{i,k|k} \quad S_{Q,k-1}]) \tag{14}$$

where $\mathbf{Q}_{k-1}^a = S_{Q,k-1} S_{Q,k-1}^T$, and

$$\boldsymbol{\chi}_{i,k|k} = \frac{1}{\sqrt{m}}\left[X_{1,k|k-1}^{a(*)} - \hat{x}_{k|k-1}^a, X_{2,k|k-1}^{a(*)} - \hat{x}_{k|k-1}^a, \ldots, X_{m,k|k-1}^{a(*)} - \hat{x}_{k|k-1}^a\right].$$

The algorithm $S = \mathrm{Tria}(A)$ means that matrix $A$ is first QR-decomposed, and a normal orthogonal matrix $B$ and an upper triangular matrix $C$ are obtained. Let $S = C^T$, and the resulting $S$ is an upper triangular matrix.

(3) Measurement update ($k = 1, 2, \ldots$)

Calculate the updated state cubature points ($i = 1, 2, \ldots, m$).

$$X_{i,k|k-1}^a = \mathbf{S}_{k|k-1}^a \xi_i + \hat{x}_{k|k-1}^a \tag{15}$$

Calculate the predicted measurement cubature points.

$$Z_{i,k|k-1} = h\left(X_{i,k|k-1}^a\right) \tag{16}$$

Estimate predictive measurements.

$$\hat{z}_{k|k-1} = \frac{1}{m}\sum_{i=1}^{m} Z_{i,k|k-1} \tag{17}$$

The estimate of the innovation covariance matrix is:

$$S_{zz,k|k-1} = \text{Tria}([Z_{k|k-1}\ S_{R,k}]) \tag{18}$$

where $R_k = S_{R,k}S_{R,k}^T$, $Z_{k|k-1} = \frac{1}{\sqrt{m}}[Z_{1,k|k-1} - \hat{z}_{k|k-1}, Z_{2,k|k-1} - \hat{z}_{k|k-1}, \ldots, Z_{m,k|k-1} - \hat{z}_{k|k-1}]$. Estimate the cross-covariance matrix:

$$\mathbf{P}_{xz,k|k-1} = \chi_{k|k-1}Z_{k|k-1}^T \tag{19}$$

Where $\chi_{k|k-1} = \frac{1}{\sqrt{m}}[X_{1,k|k-1} - \hat{x}_{k|k-1}, X_{2,k|k-1} - \hat{x}_{k|k-1}, \ldots, X_{m,k|k-1} - \hat{x}_{k|k-1}]$.

Estimate the SRCKF filter gain.

$$\mathbf{W}_k^a = \left(\mathbf{P}_{xz,k|k-1} \Big/ S_{zz,k|k-1}^T\right) \Big/ S_{zz,k|k-1} \tag{20}$$

Based on the new measurement $z_k$ at time $k$, the system state is updated.

$$\hat{x}_{k|k}^a = \hat{x}_{k|k-1}^a + W_k\left(z_k - \hat{z}_{k|k-1}\right) \tag{21}$$

The square root factor of the error covariance matrix is updated.

$$\mathbf{S}_{k|k} = \text{Tria}([\chi_{k|k-1} - W_k Z_{k|k-1}\ \ W_k S_{R,k}]) \tag{22}$$

(4) Calculation of instantaneous variance of acceleration

To achieve the recursion of the aerodynamic parameters in the homogeneous jerk model, the instantaneous variance of acceleration needs to be calculated. The $\text{diag}(E[\tilde{\dddot{\mathbf{x}}}_k\tilde{\dddot{\mathbf{x}}}_k^T])$ in Eq. (8) can be obtained directly from the state covariance matrices associated with the output of the $k$-time filter. That is, $\text{diag}(E[\tilde{\dddot{\mathbf{x}}}_k\tilde{\dddot{\mathbf{x}}}_k^T])$; $E[\tilde{\dddot{\mathbf{x}}}_k\tilde{\dddot{\mathbf{x}}}_k^T]$ is calculated as follows:

$$\dddot{\mathbf{x}} = J(x, \dot{x}, y, \dot{y}, z, \dot{z}, \mathbf{p}) \tag{23}$$

where $\dddot{\mathbf{x}} = [\ \dddot{x}\quad \dddot{y}\quad \dddot{z}\ ]^T$ is jerk vector. Construct the variable $\mathbf{x}_n = [x, \dot{x}, y, \dot{y}, z, \dot{z}, \mathbf{p}]^T$ and the state covariance matrix $\mathbf{P}_n$. Then, $\dddot{\mathbf{x}} = J(\mathbf{x}_n)$.

The state estimation value $\hat{\mathbf{x}}_n$ and covariance $\mathbf{P}_n$ are known at time $k$, and the $E[\tilde{\dddot{\mathbf{x}}}_k\tilde{\dddot{\mathbf{x}}}_k^T]$ calculation method based on the SRCKF is given by:

$$E[\tilde{\dddot{\mathbf{x}}}_k\tilde{\dddot{\mathbf{x}}}_k^T] = E[(J(\hat{x}_n + S_{n,i}\xi_i) - J(\hat{x}_n))(J(\hat{x}_n + S_{n,i}\xi_i) - J(\hat{x}_n))^T] \tag{24}$$

where $\mathbf{S}_n = \text{chol}(P_n)$ is Cholesky decomposition $\mathbf{P}_n$; $\mathbf{S}_{n,i}$ is the $i$-th line of $\mathbf{S}_n$; $n_x$ is the dimension number of $\mathbf{x}_n$; $\xi_i$ is the number $i$ basic cubature point. The covariance of the jerk estimation error vector at time $k$ can be calculated based on Eqs. (10), (13), (15), (18), and (19).

### 4.2. Model State Error Adaptive Estimation

When the tracking model is more accurate, the state covariance can reflect the state estimation error more accurately. When the model is mismatched, it will cause the tracking of the hypersonic target in the near space. Therefore, the state estimation of the target will worsen, or even diverge, resulting in a deterioration of target tracking performance. Therefore, in piecewise-constant ierk model, the state error coefficient of the tracking target is estimated by using the model mismatch detection function $D_k$ in real time. Also, the state error coefficient is transformed into the variance transformation coefficients $C_a$ and $C_J$ to drive the change of state covariance.

The model mismatch detection function is:

$$D_k = \mathbf{v}_k^T S_{zz}^{-1}\mathbf{v}_k \tag{25}$$

where $\mathbf{v}_k$ is innovation, and $S_{zz}$ is the innovation covariance of the filter output. As the position and velocity error covariance related with the jerk error covariance change relatively smoothly during

the process of updating, the actual change of the jerk error covariance is more intense than that of the position and velocity error covariance when the target is maneuvering. Therefore, $C_a$ and $C_J$ are defined by:

$$C_a = \begin{cases} q_a D_k & D_k > 3 \\ q_a & D_k \leq 3 \end{cases}, \quad C_J = \begin{cases} q_J D_k^2 & D_k > 3 \\ q_J & D_k \leq 3 \end{cases} \tag{26}$$

where $q_a$ and $q_J$ are the designed parameters, which can be obtained from simulation. Therefore, considering the model mismatch caused by target maneuver, the acceleration variance calculation method of Eq. (9) is modified as:

$$\boldsymbol{\sigma}_{ak}^2 = \begin{cases} \text{diag}\left(q_a D_k E[\tilde{\ddot{\mathbf{x}}}_k \tilde{\ddot{\mathbf{x}}}_k^T] + T^2 q_J D_k^2 E[\tilde{\dddot{\mathbf{x}}}_k \tilde{\dddot{\mathbf{x}}}_k^T]\right) & D_k > 3 \\ \text{diag}\left(q_a E[\tilde{\ddot{\mathbf{x}}}_k \tilde{\ddot{\mathbf{x}}}_k^T] + T^2 q_J E[\tilde{\dddot{\mathbf{x}}}_k \tilde{\dddot{\mathbf{x}}}_k^T]\right) & D_k \leq 3 \end{cases} \tag{27}$$

After the above derivation and correction, the state covariance, covariance of the process noise and model mismatch detection function are correlated. When the target aerodynamic parameter estimation is accurate, the covariance of the process noise will decrease due to filter characteristics. The state covariance is reduced, and the state estimation error caused by the measurement noise is also reduced. The value of the model mismatch detection function increases, thus leading to an increase of covariance of the process noise when the target aerodynamic parameter changes cause the model mismatch. Also, the increase of covariance of the process noise will increase the state covariance. Mutual stimulation between the state covariance and the covariance of the process noise will greatly increase the gain of the algorithm filter, which in turn reduces the state estimation error.

## 5. SIMULATION RESULTS AND ANALYSIS

### 5.1. The Simulation Scene

A boost-glide hypersonic vehicle has significant differences with the phase of aerodynamics and ballistic target. This paper takes a boost-glide hypersonic vehicle as the simulation analysis object, in order to verify the effectiveness of the proposed algorithm in this paper. References [10] and [11] set the target simulation initial state as $\mathbf{s}_1 = [0\,\text{km}\ \ 0\,\text{km}\ \ 40\,\text{km}\ \ 2.4\,\text{km/s}\ \ 0\,\text{km/s}\ \ 0\,\text{km/s}]^T$, and the radar deployment position $[500000\,\text{m}\ \ 0\,\text{m}\ \ 0\,\text{m}]^T$. We set the radar standard deviation of range and angle measuring noise to 30 m and 0.05°, respectively, and the sample interval is $T = 0.1\,\text{s}$. The tracking algorithm process noise variance of acceleration is set to $\sigma_{ax,k}^2 = \sigma_{ay,k}^2 = \sigma_{az,k}^2 = 5^2$. In order to fully verify the effectiveness of the proposed algorithm, three typical motion modes of hypersonic targets are designed:

**Table 1.** The simulation parameters of three motion modes.

| Types of motion modes | Attack angle | Bank angle |
|---|---|---|
| Motion mode 1 | Fixed at 10° | Fixed at 20° |
| Motion mode 2 | The amplitudes are 6.5° and 10.5°, respectively, and the period is 100 s square wave change. | Fixed at 0° |
| Motion mode 3 | Fixed at 10° | The amplitude is 20°, and the period is 100 s sine wave change. |

### 5.2. The Simulation Results

In order to verify the effectiveness of this algorithm, aerodynamic parameter augmentation model based on piecewise constant acceleration (abbreviated as PCA in the latter part of the simulation) in paper [10],

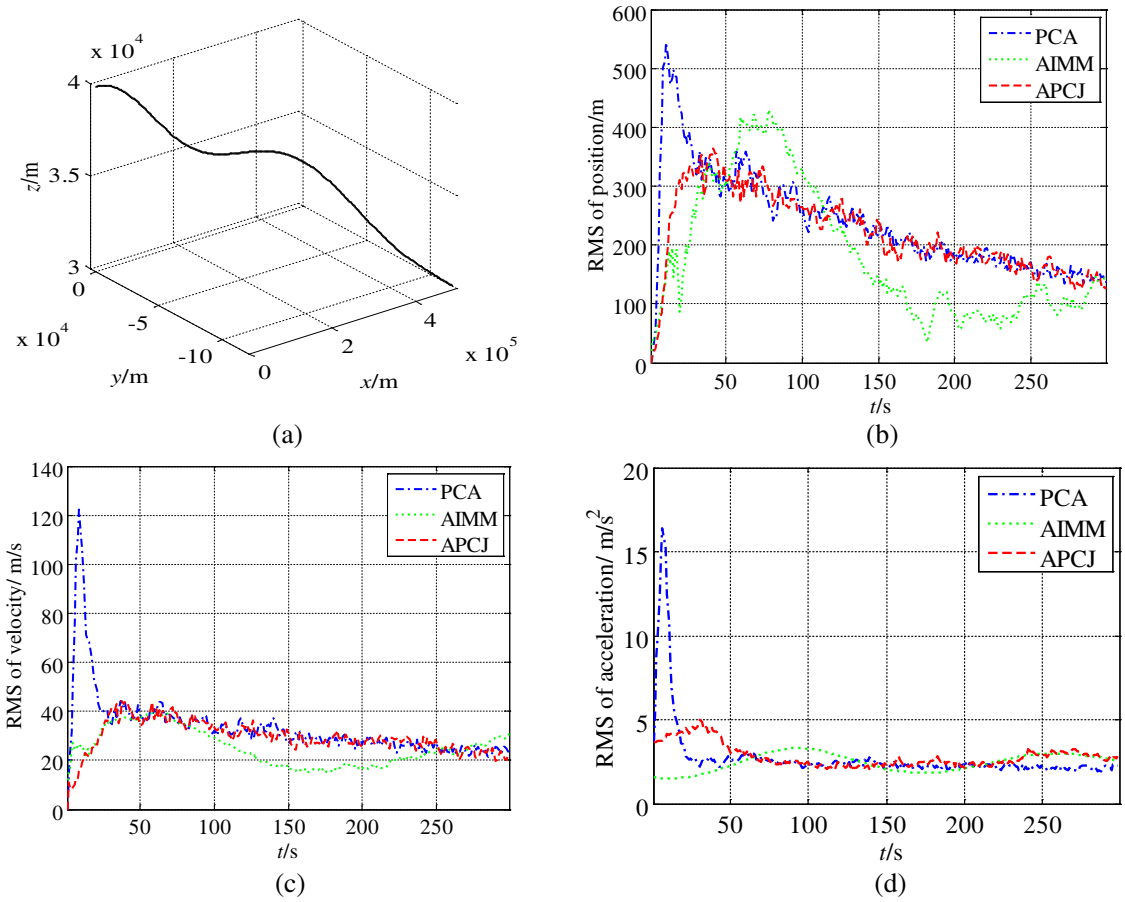


**Figure 1.** RMS of estimation error in Maneuvering Mode 1 conditions. (a) Motion path. (b) RMS of position error. (c) RMS of velocity error. (d) RMS of acceleration error.

the adaptive interactive multiple model using 10 model sets (abbreviated as AIMM in the latter part of the simulation) in paper [11] and modified piecewise constant jerk (abbreviated as APCJ in the later simulation), as proposed in this article, combined with an improved SRCKF algorithm were simulated for the previous simulation scenario. In three different maneuvering conditions, the APCJ algorithm, AIMM algorithm and PCA algorithm were used in 50 Monte Carlo simulations. The position, velocity and acceleration root mean square (RMS) errors of the three algorithms are shown in Fig. 1, Fig. 2 and Fig. 3. In the three maneuvering conditions, the tracking performance statistics and calculation time statistics of the three algorithms are shown in Table 1, Table 2 and Table 3, respectively.

From Fig. 1, Fig. 2, Fig. 3, Table 1, Table 2 and Table 3, it can be seen that in the three different cases of maneuvering modes, the adaptive tracking method based on the piecewise constant jerk model (APCJ), adaptive interactive multiple model (AIMM) and piecewise constant acceleration model (PCA)

**Table 2.** Comparison of algorithm performance in Maneuvering Mode 1.

| Types of algorithm | State Estimation Mean Error in Observation Time | | | calculating time [s] |
|---|---|---|---|---|
| | Position/[m] | Velocity/[m·s$^{-1}$] | Acceleration/[m·s$^{-2}$] | |
| APCJ | 182.04 | 26.50 | 2.01 | 1.56 |
| AIMM | 184.09 | 25.58 | 2.25 | 3.89 |
| PCA | 196.43 | 27.18 | 2.41 | 2.27 |

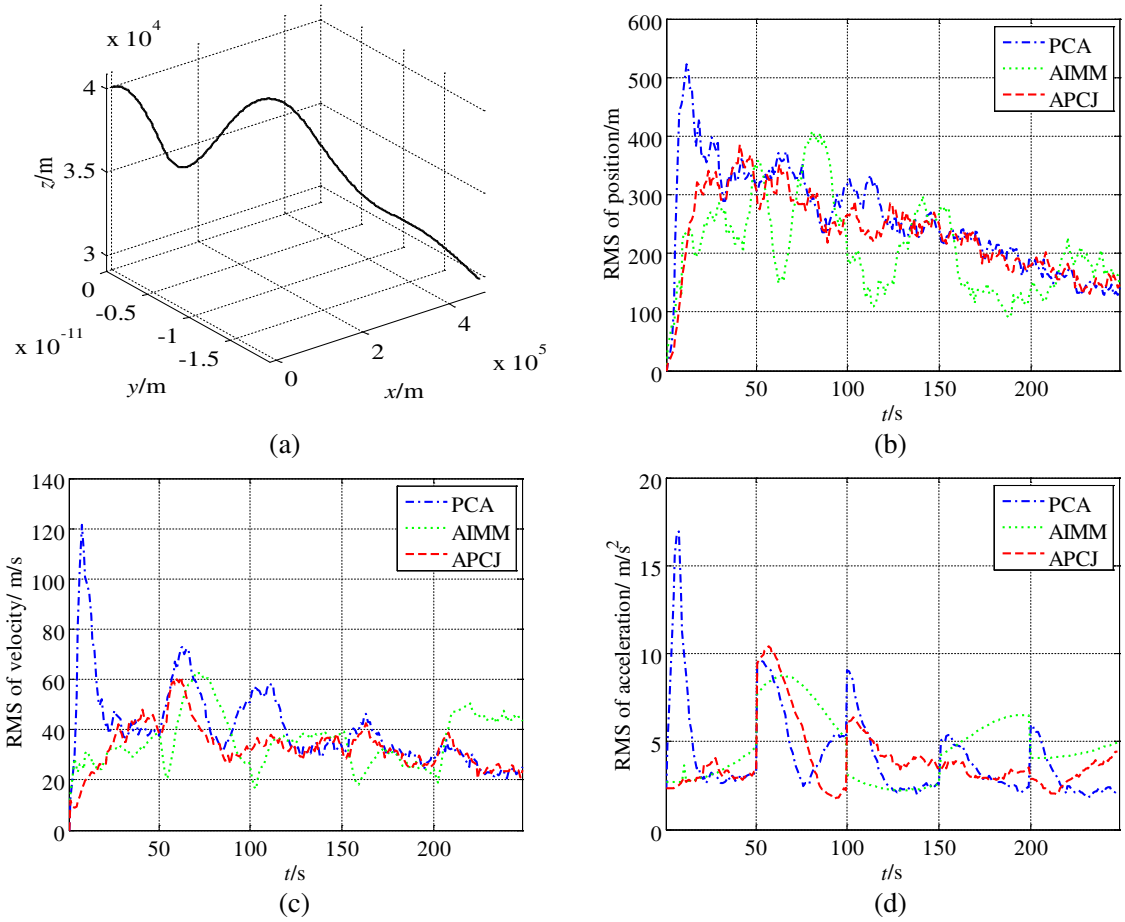


**Figure 2.** RMS of estimation error in Maneuvering Mode 2 conditions. (a) Motion path. (b) RMS of position error. (c) RMS of velocity error. (d) RMS of acceleration error.

**Table 3.** Comparison of algorithm performance in Maneuvering Mode 2.

| Types of algorithm | State Estimation Mean Error in Observation Time | | | Calculating time [s] |
|---|---|---|---|---|
| | Position/[m] | Velocity/[m·s$^{-1}$] | Acceleration/[m·s$^{-2}$] | |
| APCJ | 214.73 | 29.94 | 3.92 | 2.01 |
| AIMM | 213.62 | 35.36 | 4.01 | 3.79 |
| PCA | 232.94 | 38.35 | 4.02 | 2.29 |

**Table 4.** Comparison of algorithm performance in Maneuvering Mode 3.

| Types of algorithm | State Estimation Mean Error in Observation Time | | | Calculating time [s] |
|---|---|---|---|---|
| | Position/[m] | Velocity/[m·s$^{-1}$] | Acceleration/[m·s$^{-2}$] | |
| APCJ | 207.18 | 28.31 | 3.32 | 1.75 |
| AIMM | 219.83 | 31.96 | 3.88 | 3.91 |
| PCA | 222.53 | 34.93 | 3.53 | 2.21 |

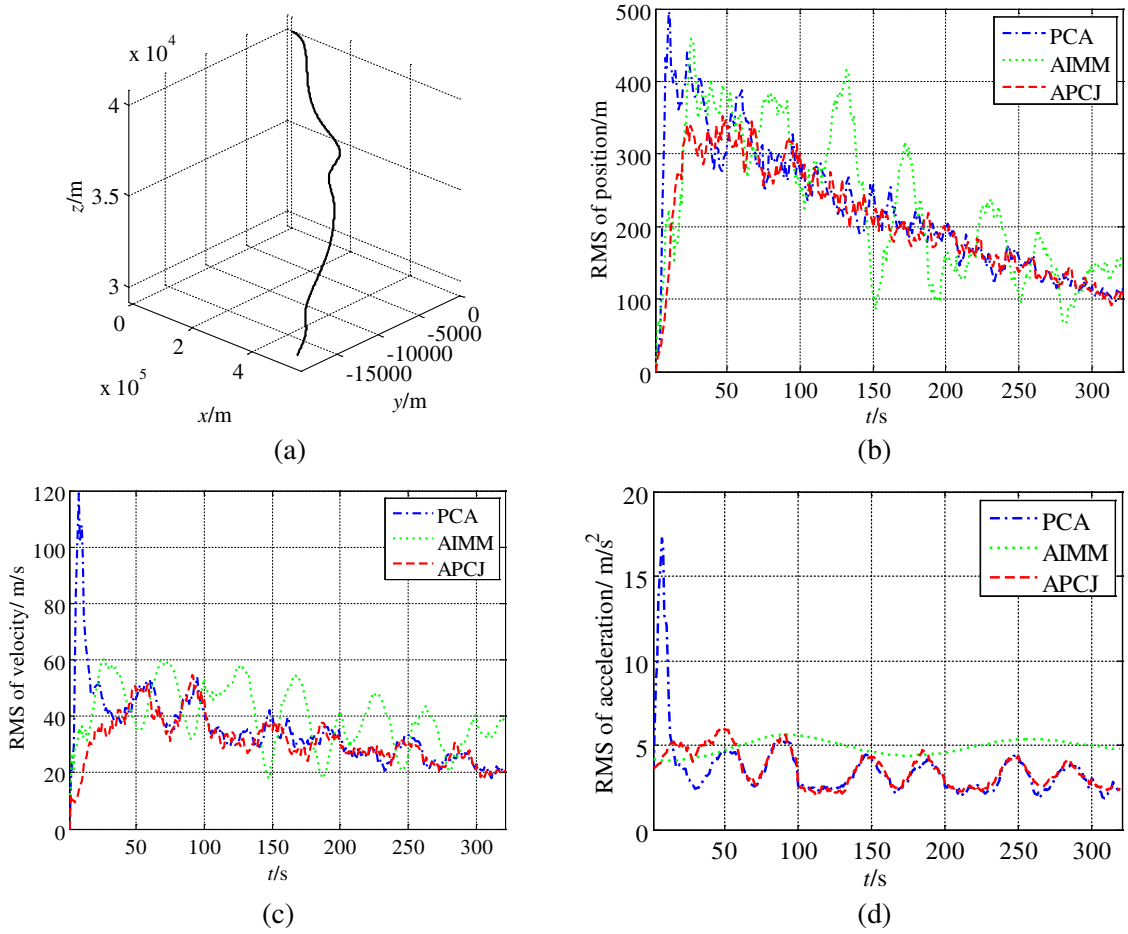


**Figure 3.** RMS of estimation error in Maneuvering Mode 3 conditions. (a) Motion path. (b) RMS of position error. (c) RMS of velocity error. (d) RMS of acceleration error.

can track the maneuvering target with a high degree of tracking accuracy. However, the APCJ algorithm has higher tracking accuracy in terms of position, velocity and acceleration. The calculation time is equivalent to the PAC algorithm, which is much lower than the AIMM algorithm. This is because the tracking algorithm of the APCJ model gives the recursive equation of acceleration, and this algorithm can update the state covariance of the system through measurement. Compared with the tracking method based on the PCA model, the convergence speed is faster and the degree of tracking accuracy is higher. However, when comparing Fig. 1 with Fig. 2 and Fig. 3, we found that, when the target is maneuvering in mode 2 and mode 3, the tracking accuracy is worse than when the target is maneuvering in mode 1. When the target flies at a fixed bank angle in mode 1, there is lateral maneuvering in its trajectory. However, the benefit is that the change in acceleration is relatively flat. On the other hand, the APCJ algorithm can adaptively adjust the gain of the filtering algorithm according to the error of the jerk dynamic model and can also compensate the acceleration estimation error in real time. As such, good tracking performance is obtained. When the target is maneuvering in mode 2 and mode 3, the acceleration of the target changes nonlinearly, which in turn increases the tracking difficulty. Because the adaptive calculation of process noise in the APCJ algorithm, compared with the PCA algorithm and AIMM algorithm, the tracking accuracy of the proposed algorithm is improved. However, the convergence speed and state estimation accuracy of the algorithm are degraded. Overall, among the three maneuvering modes, the degree of tracking accuracy based on the piecewise constant jerk model (APCJ) tracking is higher than that based on piecewise constant acceleration tracking (PCA) and the AIMM. Therefore, for hypersonic targets with high maneuvering characteristics, the tracking method

based on the segmented uniform jerk model proposed in this paper is effective. It should be noted that, although the simulation results show that the tracking effect of the APCJ algorithm is better than that of the AIMM algorithm selected in this paper, this does not mean that the proposed algorithm is better than the AIMM. The degree of the tracking accuracy of the AIMM is closely related to the selection of sub-models, the number of sub-models and the parameter settings. The comparison between the proposed algorithm and the AIMM algorithm only shows that the proposed algorithm has tracking accuracy that is similar in degree to the AIMM, which greatly reduces the degree of computational complexity.

## 6. CONCLUSION

In this paper, the dynamic model of a near pace hypersonic target (NSHT) is modeled, based on the analysis of the aerodynamic characteristics of NSHT. Thus, the piecewise adaptive jerk tracking model is established, in order to accomplish the track of the NSHT with the improved square root cubature Kalman algorithm. The simulation results show that near space target tracking can be finished more effectively. Also, the proposed method is more precise in hypersonic tracking in near space than the segmental uniform acceleration model and the AIMM. Moreover, the proposed method increases the convergence performance and stability of the state tracking, especially when the target has lateral maneuvers. This algorithm is also effective in different simulation scenarios.

## ACKNOWLEDGMENT

This paper is supported by the National Natural Science Fundation of China (No. 61503408).

## REFERENCES

1. Huang, W., S. B. Luo, and Z. G. Wang, "Key techniques and prospect of near-space hypersonic vehicle," *Journal of Astronautics*, Vol. 31, No. 5, 1259–1265, 2010.
2. Li, S. Y., L. X. Ren, Q. G. Song, et al., "Overview of anti-hypersonic weapon in near space," *Modern Radar*, Vol. 36, No. 6, 13–18, 2014.
3. Nie, W. S., S. B. Luo, and S. J. Feng, "Analysis of key technologies and development trend of near space vehicle," *Journal of National University of Defense Technology*, Vol. 34, No. 2, 107–113, 2012.
4. Hu, Z. D., Y. Cao, and S. F. Zhang, "Trajectory performance analysis and optimization design for hypersonic skip vehicle," *Journal of Astronautics*, Vol. 29, No. 3, 821–825, 2008.
5. Wang, L. D., Y. H. Zeng, L. Gao, et al., "Technology status and development trend for radar detection of hypersonic target in near space," *Journal of Signal Processing*, Vol. 30, No. 1, 72–85, 2014.
6. Dai, J., J. Cheng, and R. Guo, "Research on near-space hypersonic weapon defense system and the key technology," *Journal of the Academy of Equipment Command & Technology*, Vol. 21, No. 3, 58–61, 2010.
7. Li, X. R. and V. P. Jilkov, "Survey of maneuvering target tracking. Part II: Motion models of ballistic and space targets," *IEEE Transactions on Aerospace and Electronic Systems*, Vol. 46, No. 1, 96–119, 2010.
8. Wu, N. and L. Chen, "Adaptive kalman filtering for trajectory estimation of hypersonic glide reentry vehicles," *Acta Aeronautica et Astronautica Sinica*, Vol. 34, No. 8, 1960–1971, 2013.
9. Li, H. N., H. M. Lei, D. L. Zhai, et al., "Tracking oriented dynamics modeling of air-breathing hypersonic vehicles," *Acta Aeronautica et Astronautica Sinica*, Vol. 35, No. 6, 1651–1664, 2014.
10. Zhai, D. L., H. M. Lei, H. N. Li, et al., "Trajectory prediction oriented aerodynamic performances analysis of hypersonic vehicles," *Journal of Solid Rocket Technology*, Vol. 40, No. 1, 115–120, 2017.
11. Zhai, D. L., H. M. Lei, J. Li, et al., "Trajectory prediction of hypersonic vehicle based on adaptive IMM," *Acta Aeronautica et Astronautica Sinica*, Vol. 37, No. 11, 3466–3475, 2016.

12. Arasaratnam, S. Haykin, and R. J. Elliot, "Cubature Kalman filters," *IEEE Trans. on Automatic Control*, Vol. 54, No. 6, 1254–1269, 2009.
13. Mu, J. and Y. L. Cai, "Iterated cubature Kalman filter and its application," *Systems Engineering and Electronics*, Vol. 33, No. 7, 1454–1457, 2011.
14. Wang, P., W. X. Xie, Z. X. Liu, et al., "Performance evaluation of several methods for tracking a ballistic object," *Journal of Shenzhen University Science and Engineering*, Vol. 29, No. 5, 392–398, 2012.
15. Li, X. R. and V. P. Jilkov, "A survey of maneuvering target tracking: Approximation techniques for nonlinear filtering," *Proceeding of 2004 SPIE Conference on Signal and Data Processing of Small Targets*, 537–550, 2004.